

1 RRH: CRETACEOUS/PALEOGENE BOUNDARY

2 LRH: LEIGHTON ET AL.

3  
4 TIMING RECOVERY AFTER THE CRETACEOUS/PALEOGENE BOUNDARY:  
5 EVIDENCE FROM BRAZOS RIVER, TEXAS  
6

7 ANDREW D. LEIGHTON<sup>1</sup>, MALCOLM B. HART<sup>1,4</sup>, CHRISTOPHER W. SMART<sup>1</sup>,  
8 MELANIE J. LENG<sup>2</sup> AND MATTHEW HAMPTON<sup>3</sup>  
9

10 <sup>1</sup>School of Geography, Earth and Environmental Sciences, Plymouth University, Plymouth, PL4  
11 8AA, UK

12 <sup>2</sup>NERC Isotope Geosciences Facilities, British Geological Survey, Nottingham NG12 5GG, UK  
13 & School of Geography, University of Nottingham, University Park, Nottingham NG7 2RD, UK

14 <sup>3</sup>Network Stratigraphic Consulting Ltd, Harvest House, Cranborne Road, Potters Bar,  
15 Hertfordshire EN6 3JF, UK

16 <sup>4</sup>Correspondence author E-mail: mhart@plymouth.ac.uk  
17  
18

19  
20 ABSTRACT  
21

22 As part of an on-going re-assessment of the Cretaceous/Paleogene boundary in the  
23 Brazos River area, Falls County, Texas, a number of new exposures have been described. One of  
24 these, at Riverbank South, provides a near-continuous record of the lowermost Paleocene. It is  
25 from this succession that stable isotope analysis of bulk organic matter ( $\delta^{13}\text{C}$  and C/N) and  
26 mono-specific samples of the benthic foraminifera *Lenticulina rotulata* Lamarck ( $\delta^{18}\text{O}$  and  $\delta^{13}\text{C}$ )  
27 yields an orbitally-tuned stable isotope record, which allows the timing of events adjacent to the  
28 Cretaceous/Paleogene boundary to be determined. Using this cyclicity, it is suggested that the  
29 on-set of biotic recovery began ~40,000 years after the impact (near the base of Zone P $\alpha$ ) and  
30 that more significant recovery of planktic foraminifera and calcareous nannofossils began close  
31 to the base of Zone P1a, some 85,000–100,000 years post-impact. The data also appear to record  
32 the presence of the earliest Paleocene DAN-C2 and Lower C29n hyperthermal events and that  
33 these events appear to be an accentuated segment of this orbital cyclicity.

## INTRODUCTION

The Cretaceous/Paleogene (K/Pg) mass extinction event is not the most severe of the major extinction events in Earth's history but it is one of the most studied (Twitchett, 2006). There were synchronous extinctions (Keller et al., 2009) in both the marine and terrestrial realms including some invertebrates (e.g., ammonites), calcareous nannofossils, planktic foraminifera and non-avian dinosaurs. A bolide impact at Chicxulub in the Yucatan Peninsula, Mexico, is now generally accepted as a major cause of the extinction event (MacLeod et al., 2007), despite on-going discussions (Schulte et al., 2010) regarding the timing of the extinctions and the changes to global climate caused by the eruption of the Deccan volcanic centre in India (Adate et al., 2014; Keller, 2014; Punekar et al., 2014).

The K/Pg boundary on the Brazos River and its tributaries in Falls County, Texas (Fig. 1) has been extensively studied (Hansen et al., 1987; Yancey, 1996; Keller et al., 2009; Adate et al., 2011; Hart et al., 2011, 2012) although there are on-going debates over the placement of the boundary event in that area. Many of the discussions relate to the nature of the boundary complex exposed in the Brazos River area, which has been interpreted as either tsunami deposits associated with the Chicxulub impact (Bourgeois et al., 1988; Keller et al., 2003, 2009), a series of storm deposits (Gale, 2006) or a succession of storm deposits resting on a tsunami-generated erosion surface (Yancey, 1996; Hart et al., 2012; Yancey & Liu, 2013). At its base, the boundary complex contains re-worked, impact-derived spherules, overlain by discrete sandstone bodies (Hart et al., 2012) with hummocky cross-stratification, climbing ripples, complex bioturbation and fossil-rich siltstone inter-beds. To date, investigations of this boundary have focused mainly

on exposures in the bed of the Brazos River close to the Rt. 413 bridge, the creeks (Darting Minnow and Cottonmouth) or cored material. Recently, a new section on the Brazos riverbank, which crops out between Cottonmouth and Darting Minnow creeks (8.5 km south of the Rt. 413 bridge), has been re-discovered and described (Plummer, 1926; Hart et al., 2012, figs. 2–4). This exposure, known as River Bank South (RBS), is laterally continuous along a >100 m long cliff and is currently the most complete exposure of the K/Pg boundary in the area at the present time (Fig. 2). There have, however, been times between 1926 and 2011 when the outcrop was covered by river-derived sediments.

The RBS succession exposes the uppermost part of the Corsicana Mudstone Formation (uppermost Maastrichtian). The volcanic ash seen in Cottonmouth Creek, 45 cm below the base of the ‘Event Bed’ (Keller et al., 2007; Hart et al., 2012) has not been recorded despite quite extensive clearance of the outcrop. This volcanic ash, fully documented by Hart et al. (2012, p. 75–77) has been recorded within the Corsicana Mudstone Formation just north of the Rt. 413 bridge at a location described as River Bank North (RBN on Fig. 1). The thickness of the Corsicana Mudstones between the volcanic ash and the tsunami-generated erosion surface is variable, as would be expected below such an erosive surface. The conglomerate of re-deposited calcareous mudstone nodules that marks the base of the ‘Event Bed’ succession in the bed of the Brazos River immediately downstream of the Rt. 413 bridge is also indicative of the levels of down-cutting by the tsunami. In Darting Minnow Creek the ‘Event Bed’ is present in the waterfall succession but, traced downstream, the Maastrichtian mudstones are directly overlain by Paleocene strata with the level of the ‘Event Bed’ represented by only an erosion surface. The absence of the ‘Event Bed’ was also recorded in the nearby Mullinax 3 core (Adatte et al., 2011; Hart et al., 2012). This level of field investigation and understanding is required prior to the

careful collection of representative suites of samples from the various localities and the subsequent micropaleontological investigations.

## METHODOLOGY

Planktic foraminifera have been extensively studied (Keller, 1989; Keller et al., 2009; Abramovich et al., 2011) in this area and they clearly demonstrate the typical K/Pg mass extinction pattern. Fewer investigations of benthic foraminifera have been undertaken (Plummer, 1926, 1931; Cushman, 1946; Hart et al., 2011; Leighton, 2014), even though they are highly diverse and abundant throughout the K/Pg boundary succession. Figure 3 shows the lithostratigraphy, nature of the sediments and some of the more important benthic foraminifera. This assemblage is typical of the Gulf Coastal Plain area (Plummer, 1926, 1931; Cushman, 1946; Olsson et al., 1996; Culver, 2003; Schulte & Speijer, 2009). As indicated by Hart et al. (2011, 2012), both the latest Maastrichtian and earliest Paleocene assemblages are typical of an inner to mid-shelf setting with a water depth of 50–100 m based on the analysis of morphotypes (see Koutsoukos & Hart, 1990). This so-called ‘Midway-type assemblage’ (Berggren & Aubert, 1975) is in contrast to the deeper-water ‘Velasco-type assemblage’ (Schnitker, 1979) that has been described from northeast Mexico (Alegret & Thomas, 2001 and references therein).

Here we report stable isotope ratios obtained from the benthic species *Lenticulina rotulata* Lamarck, an epifaunal/semi-infaunal taxon (Koutsoukos & Hart, 1990) that is abundant throughout the succession and has been used by other authors (Keller et al., 2009; Adatte et al., 2011) for stable isotope analysis at other K/Pg boundary locations. Specimens for the stable isotope analysis were obtained by normal micropaleontological processing techniques. The bulk

sediment was air dried, weighed and then soaked in white spirit (Stoddart Spirit) for ~4 hours, after which the excess white spirit was removed by filtering. Samples were then immersed in de-ionised water for ~12 hours before washing through a 45  $\mu\text{m}$  sieve, and then dried in an oven at 20°C. Once dry, the >45  $\mu\text{m}$  residues were dry sieved into the >500  $\mu\text{m}$ , 500–250  $\mu\text{m}$ , 250–150  $\mu\text{m}$  and 150–45  $\mu\text{m}$  size fractions. If the samples were not fully disaggregated the whole process was repeated 2 or even 3 times. All samples were processed in stratigraphical order.

Individual specimens of *L. rotulata* from three different size fractions were analysed to assess the isotopic variations with specimen size (= growth or ontogeny). Specimens from the >500  $\mu\text{m}$ , 500–250  $\mu\text{m}$  and 250–150  $\mu\text{m}$  size fractions were checked by both optical and electron microscopy for evidence of re-crystallization or chamber infilling. Clean specimens were weighed, as approximately 15–100 mg were required for the isotope analysis. For the >500  $\mu\text{m}$  size fraction, this equated to 2–3 individuals, while 4–6 and 9–14 individuals were needed from the 500–250  $\mu\text{m}$ , and 250–150  $\mu\text{m}$  fractions respectively. Measurements of  $\Delta^{13}\text{C}$  and  $\delta^{18}\text{O}$  were performed on a GV IsoPrime mass spectrometer plus Multiprep device, located in the National Isotope Geosciences Laboratory (NIGL), Keyworth, Nottingham. Isotope values ( $\delta^{13}\text{C}$ ,  $\delta^{18}\text{O}$ ) are reported as per mille (‰) deviations of the isotopic ratios ( $^{13}\text{C}/^{12}\text{C}$ ,  $^{18}\text{O}/^{16}\text{O}$ ) calculated to the VPDB scale using a within-run laboratory standard calibrated against NBS standards. Analytical reproducibility of the standard calcite (KCM) is < 0.1‰ for  $\delta^{13}\text{C}$  and  $\delta^{18}\text{O}$ .

After an acid wash to remove any carbonate material,  $\delta^{13}\text{C}$  and C/N were measured on the organic material by combustion in a Costech Elemental Analyser (EA) on-line to a VG Triple Trap and Optima dual-inlet mass spectrometer (also located at NIGL). Values of  $\delta^{13}\text{C}$  were calculated to the VPDB scale using a within-run laboratory standards calibrated against NBS18, NBS-19 and NBS22. Replicate analysis of well-mixed samples indicated a precision of + <0.1‰

(1 SD). Ratios of C/N were calibrated against an Acetanilide standard. Replicate analysis of well-mixed samples indicated a precision of + <0.1.

## RESULTS

The stable isotope data from *L. rotulata* are shown in Figure 4. As there is a significant degree of reworking in the lowermost Paleocene, it is possible that the first 50 cm of the Paleocene *may* include a re-worked signal from the Maastrichtian, *despite* the excellent preservation. It is evident that the large  $\delta^{13}\text{C}$  negative excursion that is often recorded immediately above the K/Pg boundary (Fig. 5) is not present in the RBS section (see Martinez-Ruiz et al., 1994; Hart et al., 2005, fig. 10; Lamolda et al., 2016, fig. 7; Hart et al., 2016, fig. 4). This is unsurprising as the global, post-impact iridium anomaly is also absent from this succession (Gertsch & Keller, 2012).

There is a full discussion of the K/Pg boundary at River Bank South given by Hart et al. (2012). Following the agreed definition of the Global Stratotype Section and Point (GSSP) provided by Molina et al. (2006), the boundary is the erosion surface generated by the tsunami that resulted from the Chicxulub impact, with the overlying spherule bed and storm-derived sandstones and siltstones representing the lowermost Paleocene. In more distal areas (from the impact) such as Stevns Klint (Denmark), the Bottacione Gorge and Contessa Highway successions near Gubbio (Italy), Gams (Austria), El Kef (Tunisia), Agost (Spain) and Caravaca (Spain) the boundary hiatus is immediately overlain by sediments containing the iridium anomaly and the negative  $\delta^{13}\text{C}$  isotope excursion (see, for example, Lamolda et al., 2016, fig. 7), neither of which are recorded in the Brazos River successions.

In the RBS succession, a series of gradually increasing, cyclical (?), stable isotope excursions are recorded up-section into the Paleocene (Fig. 4). The >500  $\mu\text{m}$  signal records these excursions well, but the amplitude of each excursion increases as the size and, therefore, maturity, of the *L. rotulata* specimens decreases. This indicates that the size (= age) of the benthic foraminifera test is inversely proportional to the  $\delta^{18}\text{O}$  and  $\delta^{13}\text{C}$  signals. The amplitude of the cyclicity in these excursions increases from the K/Pg boundary to within Zone P1a, where the largest excursions ( $\sim 6\text{‰}$  and  $>5\text{‰}$  in  $\delta^{18}\text{O}$  and  $\delta^{13}\text{C}$  respectively) in the smallest size fraction are recorded. The excursions occur in all of the size fractions in the same interval, indicating that the isotope signal appears to be genuine.

Cross-plots of  $\delta^{18}\text{O}$  and  $\delta^{13}\text{C}$  are often used extensively in paleoceanography (e.g., Wendler et al., 2013) to identify both benthic and planktic foraminifera niches (e.g., Birch et al., 2013 and references therein). In our case, only data from a single benthic taxon is used and any scatter, therefore, shows only the variability of the stable isotope signal with the size of specimens analysed (= growth).

The bulk organic  $\delta^{13}\text{C}_{\text{org}}$  is similar to the benthic foraminiferal  $\delta^{13}\text{C}_{\text{carbonate}}$  especially around the major excursions in Zone P1a (Fig. 5). Bulk  $\delta^{13}\text{C}_{\text{org}}$  shows a negative excursion of  $>1\text{‰}$ , followed by a positive excursion of  $>1\text{‰}$ . Bulk  $\delta^{13}\text{C}_{\text{org}}$  shows a cyclical pattern of positive and negative excursions, the magnitude of which increases up-section, similar to benthic foraminiferal  $\delta^{13}\text{C}_{\text{carbonate}}$ . The carbon/nitrogen (C/N) ratio increases to  $>10$  in this interval which would normally be interpreted as a greater contribution of terrestrial organic material (Fig. 5; see Sampei & Matsumoto, 2001 and Lamb et al., 2007).

There is a variable response in the foraminifera  $>500\text{ }\mu\text{m}$ ,  $500\text{--}250\text{ }\mu\text{m}$  and  $250\text{--}150\text{ }\mu\text{m}$  size fraction  $\delta^{18}\text{O}$  data, with the greatest variation within the smallest (usually the more juvenile)



specimens. This ontogenetic variation in stable isotope data in benthic foraminifera has been reported before using extant material (Schumacher et al., 2010) from the Indian Ocean, where the variation was attributed to the infaunal mode of life, with juveniles residing at a greater depth in the sediment than the larger adults. Ishimura et al. (2012) have confirmed this variation, although they used the weight (i.e., calcification) of the specimens rather than overall dimensions. In their study of living foraminifera, the lightest and, therefore, the youngest and – though not discussed – the smallest forms recorded the largest negative excursions. Wendler et al. (2013), reported a large variation in *Lenticulina* spp. stable isotope data from the Turonian (Wendler et al., 2013, fig. 6) and this was attributed to the opportunistic life-style of the genus (*op. cit.*, p. 22). These authors suggest that, for most of the benthic taxa used in their analysis, between 1 and 22 specimens were required in order to perform the stable isotope analysis. If *Lenticulina* spp. are recording significant stable isotope variability with size (both ontogenetic change and changes in life position *vis á vis* the sediment surface) then this might explain the variability recorded by Wendler et al. (2013, p. 6). As many other authors (Keller et al., 2007, 2009) have used this genus from a range of size fractions their data may have been compromised by this ontogenetic variability. This relationship has previously been described from planktic foraminifera (Bornemann & Norris, 2007; Birch et al., 2013), where individuals are known to change their position in the water column during ontogeny, but has rarely been reported in studies of benthic foraminifera.

Whilst there is a close agreement between the results of all three size fractions, it is the 250–150 µm size fraction (juveniles) that displays the greatest variability in the  $\delta^{18}\text{O}$  data (Fig. 4). These results indicate that there is a clear variation in  $\delta^{18}\text{O}$  and  $\delta^{13}\text{C}$  with size and that comparisons with data generated from ‘bulk’ or randomly selected individuals may be invalid.

The graphs in Figure 4 show that only a profile based on standardised samples can be used in a reliable way to determine events. The key features of the stable isotope data are presented below.

The lowermost Paleocene ‘large’ negative  $\delta^{13}\text{C}$  excursion (Hart et al., 2005, fig. 10; Schulte et al., 2010; Hart et al., 2016, fig. 4; Lamolda et al., 2016, fig. 7) is not evident (except perhaps in the fine fraction data: Fig. 5). This is because the reworked spherule-rich bed and the sandstones of the ‘Event Bed’ represent a disturbed environment in which the stable isotope signal has been lost by erosion or completely masked by sediment mixing. The pattern of  $\delta^{18}\text{O}$  and  $\delta^{13}\text{C}$  excursions above the ‘Event Bed’ appears cyclical and probably represents an orbital forcing. A record of orbital cyclicity is well-known in the Maastrichtian (Hart et al., 2005, fig. 9; Batenberg et al., 2012, 2014) and Paleocene (Zachos et al., 2010; Westerhold et al., 2012) and the cyclicity observed in our RBS succession is almost certainly that of the 21kyr precession signal. Although no obvious sedimentary cycles are observed in the lowermost Paleocene deposits of Texas (Fig. 2), there are distinctive carbonate-mudstone cycles recorded in the coeval Lower Paleocene sediments of the Braggs, Mussel Creek (Hart et al., 2013, fig. 7), Miller’s Ferry (Olsson et al., 1996) and Moscow Landing (Hart et al., 2013, fig. 12) successions in Alabama.

## TIMING OF EVENTS

In the chalks of the Sigerslev Member (Surlyk et al., 2006) exposed in the Stevns Klint succession, the stable isotope data (Hart et al., 2005, fig. 10) appear to record a precessional cyclicity, which was also recorded in the Maastricht chalk succession of the Netherlands (Schiøler et al., 1997) and in the Maastrichtian successions on the north coast of Spain (Batenberg et al., 2012, 2014). The ‘Grey Chalk’ (= Højerup Member) of the Stevns Klint

succession, which displays visible signs of sediment transport and the formation of ‘mounds’ on the Maastrichtian sea floor, records no cyclicity as a result of sediment mixing. The overlying Fish Clay (= Fiskeler Member), however, records (Hart et al., 2016, fig. 4) the characteristic, negative  $\delta^{13}\text{C}$  excursion (see Molina et al., 2006) and a number of other  $\delta^{13}\text{C}$  excursions that diminish in magnitude up-section (see Martinez-Ruiz et al., 1994). The total thickness of the Fish Clay may, if these are precessional cycles, represent 40,000 – 60,000 years. This interval of time is represented by only <50 cm of sediment (after compaction), implying a remarkably slow rate of sedimentation. This is, however, to be expected as – in the chalk sea of northwest Europe – a loss of calcareous nannofossils and planktic foraminifera would significantly reduce the sediment supply. The background supply of siliciclastic sediment (largely clays) normally represents <1% of uppermost Cretaceous chalks in north-west Europe (Hancock, 1976) and the loss of carbonate sediment supply following the K/Pg mass extinction event explains the reduced sedimentation rate. The Fish Clay contains a diverse and abundant assemblage of dinoflagellatecysts (Hansen, 1977; Hultberg, 1985, 1986, 1987; Hultberg & Malmgren, 1987), but this abundance must also be viewed in the context of the reduced sedimentation rate.

In Texas, however, the dominant sediment supply is siliciclastic and the stable isotope data (Fig. 4) do not show the same levels of condensation, despite a similar loss of calcareous nannofossils and planktic foraminifera at the level of the K/Pg extinction event. The large  $\delta^{13}\text{C}$  negative excursion is missing and there are, therefore, ~2 excursions prior to the P0/P $\alpha$  boundary. This indicates ~40,000 years of elapsed time between the extinction event and the onset of ‘recovery’. Berggren & Pearson (2005) have also indicated ~30,000 years for the duration of Zone P0. As there are a further 2–3 cycles to the P $\alpha$ /P1a boundary (Fig. 4), this places the on-set of a more comprehensive recovery of the plankton at ~80,000–100,000 years.

At the level of the Middle Sandstone Bed (MSB) and the Dirty Sandstone Bed (DSB) the benthic foraminifera are at their most diverse (Fig. 3) with large specimens recorded. Many of these nodosariids are exceptionally long and, as the apical spine and the aperture are often present, unlikely to have suffered any disturbance or transport. The presence of these large specimens was noted by Plummer (1926) as being a particular characteristic of the RBS section. Following the models of Emery & Myers (1996, fig. 6.14) and Oxford et al. (2000, 2004), this would suggest that the MSB/DSB interval represents a zone of maximum flooding, which may contribute to the increased  $\delta^{13}\text{C}$  peak. There is also a peak in the  $\delta^{13}\text{C}_{\text{organic}}$  record (Fig. 5), which may indicate a greater supply of terrestrial organic material and increased surface run-off from the land.

## PALEOCENE HYPERTHERMAL EVENTS

The Paleocene world was characterised by a continuing greenhouse condition and, within it, there are a number of significant – but transient – hyperthermal events (Bralower et al., 2002; Speijer, 2003; Petrizzo, 2005; Bernaola et al., 2007; Quillévéré et al., 2008; Bornemann et al., 2009; Coccioni et al., 2010). Whilst the most prominent is the Paleocene–Eocene Thermal Maximum or PETM (Zachos et al., 2001, 2010), earlier events are also quite significant and, in carbonate-rich sediments, are associated with a drop in carbonate production and/or enhanced dissolution. The DAN-C2 and Lower C29n events (Coccioni et al., 2010) have been identified in the Contessa Highway section (Gubbio, Italy) and a small number of ODP/DSDP sites (Quillévéré et al., 2008). None of these locations are in a shallow-water, mid-shelf environment, comparable with the Brazos River area. In the RBS succession the maximum  $\delta^{13}\text{C}$  excursion

appears to be coeval with the Lower C29n event while the Dan-C2 event (represented by the upper P $\alpha$  and lower P1a zones) is less pronounced.

The significant negative  $\delta^{18}\text{O}$  and  $\delta^{13}\text{C}$  excursion near the NP1/NP2 boundary approximately 2.5 m above the K/Pg boundary represents a possible  $<6^\circ\text{C}$  warming that is relatively short-lived. This appears to be coeval with the Lower C29n hyperthermal event (Coccioni et al., 2010) while a smaller, but still significant, negative  $\delta^{18}\text{O}$  and  $\delta^{13}\text{C}$  excursion below this near the P $\alpha$ /P1a boundary appears to be coeval with the DAN-C2 hyperthermal event. The DAN-C2 hyperthermal event (Quillévéré et al., 2008; Coccioni et al., 2010) occurs within the lower P1a and NP1 biozones, while the Lower C29n hyperthermal event occurs within the uppermost part of the NP1 calcareous nannofossil biozone and within the P1a planktic foraminiferal biozone. The hyperthermal events at Contessa Highway (Coccioni et al., 2010) appear coeval with the timing of the excursions in the RBS section as the biostratigraphy is well-constrained. The biostratigraphy within the RBS section is reliable and accurate, with the calcareous nannofossil data based on the same samples as those used in the analysis of the benthic and planktic foraminifera and the stable isotope analyses. The distribution of the planktic foraminifera in the RBS succession is exactly comparable to that recorded in the Brazos-1 section by Liu (pers. comm., 2012, 2013) and the Brazos River outcrop immediately south of the Rt. 413 bridge. The distribution of taxa is also in agreement with that recorded in the Mullinax-1 borehole (Abramovich et al., 2011; Keller & Adatte, 2011 and papers cited therein), though our placing of the K/Pg boundary is different to that recorded by these authors. The calcareous nannofossil data allow the placing of NP1 and NP2, with direct comparisons to the successions in Agost (Lamolda et al., 2016), Caravaca (Lamolda et al., 2005), El Kef (Pospichal, 1994) and Elles (Gardin, 2002). The magnitude of the stable isotopic excursions recorded in the Brazos

River area are larger than those observed near Gubbio (Coccioni et al., 2010), although this can be attributed to the use of species-specific benthic foraminifera within this study rather than bulk rock samples.

The  $\delta^{13}\text{C}_{\text{organic}}$  isotope data (Fig. 5) are in close agreement with the species-specific foraminiferal isotope data, with the  $\delta^{13}\text{C}_{\text{organic}}$  signal closely reflecting the excursions of the species-specific  $\delta^{13}\text{C}_{\text{carbonate}}$  isotope data. This indicates that the carbon source for both the foraminifera and the sediments ( $\delta^{13}\text{C}_{\text{organic}}$  and  $\delta^{13}\text{C}_{\text{carbonate}}$ ) is the same. An increase in the C/N ratio  $>10$  indicates a more terrestrial origin for organic material (Fig. 5). The marked increase in the C/N ratio coincides with the marked negative  $\delta^{13}\text{C}$  excursion of the foraminiferal isotopic data and suggests that there was a greater supply of terrestrial plant material and increased surface run-off from the land onto the shelf. This mechanism could also account for the fluctuations of the  $\delta^{18}\text{O}$  isotope signal as this could be marking an increase of freshwater into the system and, therefore, much lighter isotopic values. Increased surface run-off from the land, as a result of hydrological changes, is a particular feature that often characterizes hyperthermal events (see Manners et al., 2013, and references therein), so the interpretation of increased freshwater input into the Brazos River area supports this conclusion.

The general warming recorded by the DAN-C2 and Lower C29n events (Coccioni et al., 2010) appears to be associated with the interval of time close to the last of the eruption phases of the Deccan Plateau (Chenet et al., 2007, 2009), although there is an on-going re-evaluation of the ages of the Deccan volcanics (e.g., Schoene et al., 2015). The timing of the hyperthermal event(s) in the Brazos River area suggests that the DAN-C2 and Lower C29n event may be more widespread than previously suggested. The stable isotope data from the Brazos River area may be astronomically tuned, a feature of the DAN-C2 event (Quillévéré et al., 2008). An

astronomical signal has also been suggested (Jolley et al., 2011; Gilmour et al., 2012, 2013, 2014) following an analysis of the sediments within the Boltysh impact crater in Ukraine. There are four climate-induced cycles (Gilmour et al., 2013, 2014) between the K/Pg boundary and what has been identified as the DAN-C2 event. If this cyclicity, and the DAN-C2 event (and Lower C29n event), are confirmed from terrestrial, shallow marine (Brazos River area) and deeper marine successions, then these events are comparable to other Paleogene hyperthermal events that are recorded globally and from a wide range of environments (both terrestrial and marine).

## CONCLUSIONS

Stable isotope data derived from size-controlled samples of *Lenticulina rotulata* Lamarck across the K/Pg boundary in the Brazos River area, Texas, indicate that early recovery began ~40,000 years post-impact and that a more significant recovery was under-way by 80,000–100,000 years post-impact. The data also suggest that the DAN-C2 and Lower C29n hyperthermal events have been detected in the mid-shelf environment represented by the sediments of the Kincaid Formation, Brazos River area, Falls County, Texas. These events appear to be coeval with those identified from the Contessa Highway K/Pg section in Italy, and occur at the same stratigraphic level as determined by both calcareous nannofossil and planktic foraminiferal biozonation schemes. The variation in  $\delta^{18}\text{O}$  and  $\delta^{13}\text{C}$  recorded in the various size fractions of the mono-specific samples used in our investigation raises issues for stable isotope data derived from variously-sized foraminifera or samples of mixed benthic assemblages. The data do, however, indicate that fossil material is showing stable isotope variations in line with

those recorded in modern (living) foraminifera. The stable isotopic signal from the Brazos River area indicates an increased amount of surface run-off (freshwater input) in the early Paleocene. The increased surface run-off, hyperthermal events and bulk organic  $\delta^{13}\text{C}$  geochemical signals indicate that the earliest Paleocene immediately after the K/Pg boundary event was a period of climatic instability and fluctuating environmental parameters.

## ACKNOWLEDGMENTS

ADL acknowledges receipt of a Plymouth University Scholarship to support his PhD research (2009–2013). The authors also acknowledge financial support from Plymouth University, the Geological Society of London (MBH) and Shell Exploration & Production, Houston (MBH/ADL). Mr and Mrs Mullinax, owners of the Brazos Rose Ranch, are also thanked for their hospitality and un-paralleled access to their property. Prof. Tom Yancey (Texas A&M University, USA) and Prof. Rodolfo Coccioni (Urbino, Italy) are also thanked for helpful and constructive discussions. The authors acknowledge the helpful comments (and criticisms) of two reviewers that have prompted a number of improvements to the final version of the paper. Mr Tim Absalom (Plymouth University Geomapping Unit) is thanked for his assistance with some of the figures.

## REFERENCES

Abramovich, S., Keller, G., Berner, Z., Cymbalista, M., and Rak, C., 2011, Maastrichtian planktic foraminiferal biostratigraphy and paleoenvironment of Brazos River, Falls



357 County, Texas, USA, *in* Keller, G., and Adatte, T., (eds.), The end-Cretaceous mass  
 358 extinction and the Chicxulub impact in Texas: SEPM Special Publication, v. 100, p. 123–  
 359 156.

360 Adatte, T., Keller, G., and Baum, G. R., 2011, Age and origin of the Chicxulub impact and  
 361 sandstone complex, Brazos River, Texas: Evidence from lithostratigraphy and  
 362 sedimentology, *in* Keller, G., and Adatte, T. (eds.), The end-Cretaceous mass extinction  
 363 and the Chicxulub impact in Texas: SEPM Special Publication, v. 100, p. 43–80.

364 Adatte, T., Fantasia, A., Samant, B., Mohabey, D., Font, E. Keller, G., Khozyem, H., and  
 365 Gertsch, B., 2014, Deccan volcanism: a main trigger of environmental changes leading to  
 366 the K/Pg mass extinction?: *Comunicações Geológicas*, v. 101, Especial III, p. 1435–  
 367 1437.

368 Alegret, L., and Thomas, E., 2001, Upper Cretaceous and lower Paleogene benthic foraminifera  
 369 from northeastern Mexico: *Micropaleontology*, v. 47, p. 269–316.

370 Batenberg, S. J., Sprovieri, M., Gale, A. S., Hilgen, F. J., Hüsing, S., Laskar, J., Liebrand, D.,  
 371 Lirer, F., Orue-Extrebarria, X., Pelosi, N., and Smit, J., 2012, Cyclostratigraphy and  
 372 astronomical tuning of the Late Maastrichtian at Zumaia (Basque country, Northern  
 373 Spain): *Earth and Planetary Science Letters*, v. 359–360, p. 264–278.

374 Batenberg, S. J., Gale, A. S., Sprovieri, M., Hilgen, F. J., Thibault, N., Boussaha, M., Orue-  
 375 Extrebarria, X., 2014, An astronomical time scale for the Maastrichtian based on the  
 376 Zumaia and Sopelana sections (Basque country, northern Spain): *Journal of the*  
 377 *Geological Society*, London, v. 171, p. 165–180.

378 Berggren, W. A., and Aubert, J., 1975, Paleocene benthonic foraminiferal biostratigraphy,  
379 paleobiogeography and paleoecology of Atlantic-Tethyan regions: Midway-type fauna:  
380 Palaeogeography, Palaeoclimatology, Palaeoecology, v. 18, p. 73–192.

381 Berggren, W. A., and Pearson, P. N., 2005, A revised tropical to subtropical Paleogene  
382 planktonic foraminiferal zonation: Journal of Foraminiferal Research, v. 35, p. 279–298.

383 Bernaola, G., Baceta, J. I., Orue-Extebarria, X., Alegret, L., Martin-Rubio, M., Arostegui, J., and  
384 Dinarès-Turell, J., 2007, Evidence of an abrupt environmental disruption during the mid-  
385 Paleocene biotic event (Zumaia section, western Pyrenees): Geological Society of  
386 America Bulletin, v. 119, p. 785–795.

387 Birch, H., Coxall, H. K., Pearson, P. N., Kroon, D., O'Regan, M., 2013, Planktonic foraminifera  
388 stable isotopes and water column structure: Disentangling ecological signals: Marine  
389 Micropaleontology, v. 101, p. 127–145.

390 Bornemann, A., and Norris, R. D., 2007, Size-related stable isotope changes in Late Cretaceous  
391 planktic foraminifera: Implications for paleoecology and photosymbiosis: Marine  
392 Micropaleontology, v. 29, p. 32–42.

393 Bornemann, A., Schulte, P., Sprong, J., Steurbaut, E., Youssef, M., and Speijer, R. P., 2009,  
394 Latest Danian carbon isotope anomaly and associated environmental change in the  
395 Southern Tethys (Nile basin, Egypt): Journal of the Geological Society, London, v. 166,  
396 p. 135–142.

397 Bourgeois, J., Hansen, T. A., Wiberg, P. L., and Kauffman, E. G., 1988, A tsunami deposit at the  
398 Cretaceous-Tertiary boundary in Texas: Science, v. 241, p. 567–570.

399 Bralower, T. J., Premoli Silva, I., and Malone, M. J., 2002, New evidence for abrupt climate  
400 change in the Cretaceous and Paleogene: an Ocean Drilling Program expedition to  
401 Shatsky Rise, northwest Pacific: *GSA Today*, v. 12, p. 4–10.

402 Chenet, A. L., Quidelleur, X., Fluteau, F., Courtillot, V., and Bajpai, S., 2007,  $^{40}\text{K}$ – $^{40}\text{Ar}$  dating of  
403 the Main Deccan large igneous province: Further evidence of KTB age and short  
404 duration: *Earth and Planetary Science Letters*, v. 263, p. 1–15.

405 Chenet, A. L., Courtillot, V., Fluteau, F., Gerard, M., Quidelleur, X., Khadri, S. F. R., Subbaro,  
406 K. V., and Thordarson, T., 2009, Determination of rapid Deccan eruptions across the  
407 Cretaceous-Tertiary boundary using paleomagnetic secular variation: 2. Constraints from  
408 analysis of eight new sections and synthesis for a 3500 m-thick composite section:  
409 *Journal of Geophysical Research*, v. 114, B06103, DOI:10.1029/2008JB005644

410 Coccioni, R., Frontalini, F., Bancalà, G., Fornaciari, E., Jovane, L., and Sprovieri, M., 2010, The  
411 Dan-C2 hyperthermal event at Gubbio (Italy): Global implications, environmental  
412 effects, and cause(s): *Earth and Planetary Science Letters*, v. 297, p. 298–305.

413 Culver, S. J., 2003, Benthic foraminifera across the Cretaceous–Tertiary (K–T) boundary: A  
414 review: *Marine Micropaleontology*, v. 47, p. 177–226.

415 Cushman, J. A., 1946, Upper Cretaceous foraminifera of the Gulf Coastal region of the United  
416 States and adjacent areas: United States Geological Survey, Professional Paper, no. 206,  
417 241 p.

418 Emery, D., and Myers, K. J., 1996, *Sequence Stratigraphy*: Blackwell Science, Oxford, 297 p.

419 Gale, A. S., 2006, The Cretaceous-Paleogene boundary on the Brazos River, Falls County,  
420 Texas: Is there evidence for impact-induced tsunami sedimentation?: *Proceedings of the*  
421 *Geologists' Association*, London, v. 117, p. 173–185.

422 Gardin, S., 2002, Late Maastrichtian to early Danian calcareous nannofossils at Elles (Northwest  
 423 Tunisia). A tale of one million years across the K-T boundary: *Palaeogeography,*  
 424 *Palaeoclimatology, Palaeoecology*, v. 178, p. 211–231.

425 Gertsch, B., and Keller, G., 2012, Platinum group element (PGE) geochemistry of Brazos  
 426 sections, Texas, USA, *in* Keller, G., and Adatte, T. (eds.), *The end-Cretaceous mass*  
 427 *extinction and the Chicxulub impact in Texas*, *SEPM Special Publication*, v. 100, p. 227–  
 428 249.

429 Gilmour, I., Jolley, D. J. W., Daley, R. J., Kelley, S. P., and Gilmour, M. A., 2012, A complete  
 430 high resolution record of the Dan-C2 hyperthermal event in the lacustrine sediments of  
 431 the Boltysh Impact Crater. *Geophysical Research Abstracts*, v. 14, EGU2012-7870-2  
 432 [abstract].

433 Gilmour, I., Gilmour, M., Jolley, D., Kelly, S., Kemp, D., Daly, R., and Watson, J., 2013, A  
 434 high-resolution nonmarine record of an early Danian hypothermal event, Boltysh crater,  
 435 Ukraine: *Geology*, v. 41, p. 783–786.

436 Gilmour, I., Jolley, D., Kemp, D., Kelley, S., Gilmour, M., Daly, R., and Widdowson, M., 2014,  
 437 *The early Danian hyperthermal event at Boltysh (Ukraine): Relation to Cretaceous-*  
 438 *Paleogene boundary events*, *in* Keller, G., and Kerr, A. C. (eds.), *Volcanism, Impacts,*  
 439 *and Mass Extinctions: Causes and Effects: Geological Society of America, Special Paper*  
 440 *No. 505*, p. 133–146.

441 Hancock, J. M., 1976, *The petrology of the chalk: Proceedings of the Geologists' Association,*  
 442 *London*, v. 86, p. 499–535 [for 1975].

443 Hansen, J. M., 1977, Dinoflagellate stratigraphy and echinoid distribution in Upper  
 444 Maastrichtian and Danian deposits from Denmark: Bulletin of the Geological Society of  
 445 Denmark, v. 26, p. 1–26.

446 Hansen, T. A., Farrand, B. R., Montgomery, H. A., Billman, H. G., and Blechschmidt, G., 1987,  
 447 Sedimentology and extinction patterns across the Cretaceous-Tertiary boundary interval  
 448 in east Texas: Cretaceous Research, v. 8, p. 229–252.

449 Hart, M. B., Feist, S. E., Håkansson, E., Heinburg, C., Price, G. D., Smart, C. W., and  
 450 Watkinson, M. P., 2005, The Cretaceous-Palaeogene boundary succession at Stevns  
 451 Klint, Denmark: Foraminifers and stable isotope stratigraphy: Palaeogeography,  
 452 Palaeoclimatology, Palaeoecology, v. 224, p. 6–26.

453 Hart, M. B., Searle, S. R., Feist, S. E., Leighton, A. D., Price, G. D., Smart, S. W., and Twitchett,  
 454 R. J., 2011, The distribution of benthic foraminifera across the Cretaceous-Paleogene  
 455 boundary in Texas (Brazos River) and Denmark (Stevns Klint), *in* Keller, G., and Adatte,  
 456 T. (eds.), The end-Cretaceous mass extinction and the Chicxulub impact in Texas: SEPM  
 457 Special Publication, v. 100, p. 179–196.

458 Hart, M. B., Yancey, T. E., Leighton, A. D., Miller, B., Liu, C., Smart, C. W., and Twitchett, R.  
 459 J., 2012, The Cretaceous-Paleogene boundary on the Brazos River, Texas: new  
 460 stratigraphic sections and revised interpretations: Journal of the Gulf Coast Association  
 461 of Geological Societies, v. 1, p. 69–80.

462 Hart, M. B., Harries, P. J., and Cárdenas, A. L., 2013, The Cretaceous/Paleogene boundary  
 463 events in the Gulf Coast: Comparisons between Alabama and Texas: Gulf Coast  
 464 Association of Geological Societies, Transactions, v. 63, p. 235–255.

465 Hart, M. B., FitzPatrick, M. E. J., and Smart, C. W., 2016, The Cretaceous/Paleogene boundary:  
 466 Foraminifera, sea grasses, sea level change and sequence stratigraphy: *Palaeogeography,*  
 467 *Palaeoclimatology, Palaeoecology*, v. 441, p. 420–429.

468 Hultberg, S. U., 1985, Dinoflagellate studies of the Upper Maastrichtian and Danian in southern  
 469 Scandinavia: University of Stockholm, unpublished PhD Thesis, 189p.

470 Hultberg, S. U., 1986, Danian dinoflagellate zonation, the C-T boundary and the stratigraphical  
 471 position of the fish clay in southern Scandinavia: *Journal of Micropalaeontology*, v. 5, p.  
 472 37–47.

473 Hultberg, S. U., 1987, Palynological evidence for a diachronous low-salinity event in the C-T  
 474 boundary clay at Stevns Klint, Denmark: *Journal of Micropalaeontology*, v. 6, p. 35–40.

475 Hultberg, S. U., and Malmgren, B. A., 1987, Quantitative biostratigraphy based on Late  
 476 Maastrichtian dinoflagellates and planktonic foraminifera from Southern Scandinavia:  
 477 *Cretaceous Research*, v. 8, p. 211–228.

478 Ishimura, T., Tsunogai, U., Hasegawa, S., Nakagawa, F., Oi, T., Kitazato, H., Suga, H., and  
 479 Toyofuku, T., 2012, Variation in stable carbon and oxygen isotopes of individual benthic  
 480 foraminifera: Tracers for quantifying the magnitude of isotopic disequilibrium:  
 481 *Biogeosciences*, v. 9, p. 4353–4367.

482 Jolley, D., Gilmour, I., Gurov, E., Kelley, S., and Watson, J., 2011, Two large meteorite impacts  
 483 at the Cretaceous-Paleogene boundary: *Geology*, v. 38, p. 835–838.

484 Keller, G., 1989, Extended Cretaceous/Tertiary boundary extinctions and delayed population  
 485 change in planktonic foraminifera from Brazos River, Texas: *Paleoceanography*, v. 4, p.  
 486 287–332.

487 Keller, G., 2014, Deccan volcanism, the Chicxulub impact, and the end-Cretaceous mass  
 488 extinctions: Coincidences? Cause and effect? *in* Keller, G., and Kerr, A. C. (eds.),  
 489 Volcanism, Impacts, and Mass Extinctions: Causes and Effects: Geological Society of  
 490 America, Special Paper No. 505, p. 57–90.

491 Keller, G., Stinnesbeck, W., Adatte, T., and Stüben, D., 2003, Multiple impacts across the  
 492 Cretaceous-Tertiary boundary: *Earth Science Reviews*, v. 62, p. 327–363.

493 Keller, G., Adatte, T., Berner, Z., Harting, M., Baum, G., Prauss, M., Tantawy, A., and Stüben,  
 494 D., 2007, Chicxulub impact predates K–T boundary: New evidence from Brazos, Texas:  
 495 *Earth and Planetary Science Letters*, v. 255, p. 339–356.

496 Keller, G., Adatte, T., Berner, Z., Pardo, A., and Lopez-Oliva, L., 2009, Age and biotic effects of  
 497 the Chicxulub impact in Mexico: *Journal of the Geological Society, London*, v. 166, p.  
 498 393–411.

499 Koutsoukos, E. A. M., and Hart, M. B., 1990, Cretaceous foraminiferal morphogroup  
 500 distribution patterns, palaeocommunities and trophic structures: A case study from the  
 501 Sergipe Basin, Brazil: *Transactions of the Royal Society, Edinburgh, Earth Sciences*, v.  
 502 81, p. 221–246.

503 Lamb, A. L., Vane, C. H., Wilson, G. P., Rees, J. G., and Moss-Hayes, V. L., 2007, Assessing  
 504  $\delta^{13}\text{C}$  and C/N ratios from organic material in archived cores as Holocene sea level and  
 505 palaeoenvironmental indicators in the Humber Estuary, UK: *Marine Geology*, v. 244, p.  
 506 109–128.

507 Lamolda, M. A., Melinte, M. C., and Kaiho, K., 2005, Nannofloral extinction and survivorship  
 508 across the K-Pg boundary at Caravaca, southeastern Spain. *Palaeogeography,*  
 509 *Palaeoclimatology, Palaeoecology*, v. 224, p. 27–52.

510 Lamolda, M. A., Melinte-Dobrinescu, M. C., and Kaiho, K., 2016, Calcareous nannoplankton  
 511 assemblage changes linked to paleoenvironmental deterioration and recovery across the  
 512 Cretaceous-Paleogene boundary in the Betic Cordillera (Agost, Spain): *Palaeogeography,*  
 513 *Palaeoclimatology, Palaeoecology*, v. 441, p. 438–452.

514 Leighton, A. D., 2014, Benthic foraminiferal change and depositional history across the  
 515 Cretaceous–Paleogene (K/Pg) boundary in the Brazos River area, Texas: Plymouth  
 516 University Research Theses, unpublished PhD Thesis (available on the PEARL website).

517 MacLeod, K. G., Whitney, D. L., Huber, B. T., and Koeberl, C., 2007, Impact and extinction in  
 518 remarkably complete Cretaceous-Tertiary boundary sections from Demerara Rise,  
 519 tropical western North Atlantic: *Geological Society of America Bulletin*, v. 119, p. 101–  
 520 115.

521 Manners, H. R., Grimes, S. T., Sutton, P. A., Domingo, L., Leng, M. J., Twitchett, R. J., Hart, M.  
 522 B., Dunkley Jones, T., Pancost, R. D., Duller, R., and Lopez-Martinez, N., 2013,  
 523 Magnitude and profile of organic carbon isotope records from the Paleocene–Eocene  
 524 Thermal Maximum: Evidence from northern Spain: *Earth and Planetary Science Letters*,  
 525 v. 376, p. 220–230.

526 Martinez-Ruiz, F., Bernasconi, S., and McKenzie, J. A., 1994, Paleooceanographic changes across  
 527 the Cretaceous-Tertiary boundary: carbon and nitrogen isotope stratigraphy:  
 528 *Mineralogical Magazine*, v. 58, p. 561–562.

529 Molina, E., Alegret, L., Arenillas, I., Arz, J. A., Gallala, N., Hardenbol, J., Von Salis, K.,  
 530 Steurbaut, E., Vandenberghe, N., and Zaghib-Turki, D., 2006, The global boundary  
 531 stratotype section and point for the base of the Danian Stage (Paleocene, Paleogene,



532 “Tertiary”, (Cenozoic) at El Kef, Tunisia – original definition and revision: *Episodes*, v.  
533 29, p., 263–278.

534 Olsson, R. K., Liu, C., and van Fossen, M., 1996, The Cretaceous-Tertiary catastrophic event at  
535 Miller’s Ferry, Alabama, *in* Ryder, G. et al. (eds.), *The Cretaceous-Tertiary boundary*  
536 *event and other catastrophes in earth history: Geological Society of America, Special*  
537 *Paper 307, Boulder, Colorado*, p. 263–277.

538 Oxford, M. J., Hart, M. B., and Watkinson, M. P., 2000, Micropalaeontological investigations of  
539 the Oxford Clay: *Geoscience in south-west England*, v. 10, p. 9–13.

540 Oxford, M. J., Hart, M. B., and Watkinson, M. P., 2004, Foraminiferal characterization of mid-  
541 Upper Jurassic sequences in the Wessex Basin (United Kingdom): *Rivista Italiana di*  
542 *Paleontologia e Stratigrafia*, v. 110, p. 209–218.

543 Petrizzo, M. R., 2005, An early late Paleocene event on Shatsky Rise, northwest Pacific Ocean  
544 (ODP Leg 198): Evidence for planktonic foraminiferal assemblage, *in* Bralower, T.J.,  
545 Premoli Silva, I., & Malone, M.J. (Eds.), *Proceedings of the Ocean Drilling Program,*  
546 *Scientific Results*, v. 198, p. 1–29.

547 Plummer, H. J., 1926, *Foraminifera of the Midway Formation in Texas: University of Texas,*  
548 *Bulletin*, no. 2644, 201 p.

549 Plummer, H. J., 1931, Some Cretaceous foraminifera in Texas: *University of Texas Bulletin*, no.  
550 3101, p. 109–203.

551 Pospichal, J. J., 1994, Calcareous nannofossils at the K-Pg boundary El Kef, Tunisia: no  
552 evidence for stepwise, gradual or sequential extinctions: *Geology*, v. 22, p. 99–102.

553 Puneekar, J., Mateo, P., and Keller, G., 2014, Effects of Deccan volcanism on paleoenvironment  
554 and planktonic foraminifera: A global survey, *in* Keller, G., and Kerr, A. C. (eds.)

555           Volcanism, Impacts, and Mass Extinctions: Causes and Effects: Geological Society of  
556           America, Special Paper No. 505, p. 91–116.

557   Quillévéré, F., Norris, R. D., Kroon, D., and Wilson, P. A., 2008, Transient ocean warming and  
558           shifts in carbon reservoirs during the early Danian: *Earth and Planetary Science Letters*,  
559           v. 265, p. 600–615.

560   Sampei, Y., and Matsumoto, E., 2001, C/N ratios in a sediment core from Nakaumi Lagoon,  
561           southwest Japan – usefulness as an organic source indicator: *Geochemical Journal*, v. 35,  
562           p. 189–205.

563   Schiøler, P., Brinkhuis, H., Roncaglia, L., and Wilson, G. J., 1997, Dinoflagellate biostratigraphy  
564           and sequence stratigraphy of the type Maastrichtian (Upper Cretaceous), ENCI quarry,  
565           The Netherlands: *Marine Micropaleontology*, v. 31, p. 65–95.

566   Schnitker, D., 1979, Cenozoic deep water benthic foraminifers, Bay of Biscay, *in* Montadert, L.  
567           et al. (eds.), Initial Reports of the Deep Sea Drilling project, U.S. Government Printing  
568           Office, Washington D.C., v. 48, p. 377–414.

569   Schoene, B., Samperton, K. M., Eddy, M. P., Keller, G., Adatte, T., Bowring, S. A., Khadri, S. F.  
570           R., and Gertsch, B., 2015, U-Pb geochronology of the Deccan Traps and relation to the  
571           end-Cretaceous mass extinction: *Science*, v. 347, p. 182–184.

572   Schulte, P., and Speijer, R., 2009, Late Maastrichtian-Early Paleocene sea level and climate  
573           changes in the Antioch Church Core (Alabama, Gulf of Mexico margin, USA): a multi-  
574           proxy approach: *Geologica Acta*, v. 7, 11–34.

575   Schulte, P., and 40 additional authors, 2010, The Chicxulub asteroid impact and mass extinction  
576           at the Cretaceous-Paleogene boundary: *Science*, v. 327, p. 1214–1218.

577 Schumacher, S., Jorissen, F. J., Mackensen, A., Gooday, A. J., and Pays, O., 2010, Onogenetic  
 578 effects on stable carbon and oxygen isotopes in tests of live (Rose Bengal stained)  
 579 benthic foraminifera from the Pakistan continental margin: *Marine Micropaleontology*, v.  
 580 76, p. 92–103.

581 Speijer, R. P., 2003, Danian–Selandian sea-level change and biotic excursion on the southern  
 582 Tethyan margin (Egypt), *in* Wings, S. L. et al. (eds.), *Causes and consequences of*  
 583 *globally warm climates in the Early Paleogene*: Geological Society of America, Special  
 584 Paper, v. 369, p. 275–290.

585 Surlyk, F., Damholt, T., and Bjerager, M., 2006, Stevns Klint, Denmark: Uppermost  
 586 Maastrichtian chalk, Cretaceous–Tertiary boundary, and lower Danian bryozoans mound  
 587 complex: *Bulletin of the Geological Society of Denmark*, v. 54, p. 1–48.

588 Twitchett, R. J., 2006, The palaeoclimatology, palaeoecology and palaeoenvironmental analysis  
 589 of mass extinction events: *Paleogeography, Palaeoclimatology, Palaeoecology*, v. 232, p.  
 590 190–213.

591 Wendler, I., Huber, B. T., MacLeod, K. G., and Wendler, J. E., 2013, Stable oxygen and carbon  
 592 isotope systematic of exquisitely preserved Turonian foraminifera from Tanzania –  
 593 understanding isotopic signature in fossils: *Marine Micropaleontology*, v. 102, p. 1–33.

594 Westerhold, T., Röhl, U., and Laskar, J., 2012, Time scale controversy: Accurate orbital  
 595 calibration of the early Paleogene: *Geochemistry, Geophysics, Geosystems*, v. 13,  
 596 Q06015, DOI: 10.1029/2012GC004096

597 Yancey, T. E., 1996, Stratigraphy and depositional environments of the Cretaceous-Tertiary  
 598 boundary complex and basal Paleocene section, Brazos River, Texas: *Transactions of the*  
 599 *Gulf Coast Association of Geological Societies*, v. 46, p. 433–442.

600 Yancey, T. E., and Liu, C., 2013, Impact-induced sediment deposition on an offshore, mud  
601 substrate continental shelf, Cretaceous-Paleogene boundary, Brazos River, Texas, USA:  
602 Journal of Sedimentary Research, v. 83, p. 354–367.

603 Zachos, J. C., Pagani, M., Sloan, L., Thomas, E., and Billups, K., 2001, Trends, rhythms, and  
604 aberrations in global climate 65 Ma to present: Science, v. 292, p. 686–693.

605 Zachos, J. C., McCarren, H., Murphy, B., Röhl, U., and Westerhold, T., 2010, Tempo and scale  
606 of late Paleocene and early Eocene carbon isotope cycles: Implications for the origin of  
607 hyperthermals: Earth and Planetary Science Letters, v. 299, p. 242–249.

608

609 *Received 25 March 2015*

610 *Accepted 22 March 2017*

611

FIGURE CAPTIONS

FIGURE 1. Locality map of the Brazos River area, Falls County, Texas (after Hart et al., 2012).

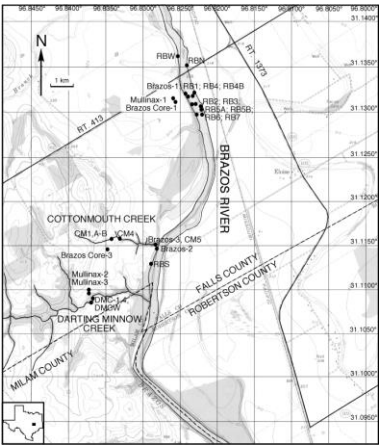
FIGURE 2. Sedimentary log of the K/Pg boundary succession exposed on the Brazos River at RBS (based on Hart et al., 2012). The thin volcanic ash recorded in the uppermost Maastrichtian of the Cottonmouth Creek succession (Hart et al., 2012) has not been recorded in the RBS succession, despite digging into the Maastrichtian mudstones as far as river levels allowed.

FIGURE 3. Sedimentary log of the RBS succession, which also shows examples of a representative selection of benthic foraminifera. The lithological symbols are explained in Figure 2 and the bed names follow Yancey (1996) including, from bottom to top, Hummocky Cross-Stratification (HCS), Lower Calcareous Horizon (LCH), Middle Sandstone Bed (MSB), Dirty Sandstone Bed (DSB), Upper Calcareous Horizon (UCH) and Rusty Pyrite Horizon (RPH).

FIGURE 4. Comparison of the  $\delta^{18}\text{O}$  and  $\delta^{13}\text{C}$  stable isotope data derived from an analysis of *Lenticulina rotulata* Lamarck in the >500  $\mu\text{m}$ , 500–250  $\mu\text{m}$  and 250–150  $\mu\text{m}$  size fractions. The thinner black line marks the running average.

FIGURE 5. Bulk organic  $\delta^{13}\text{C}$ , fine fraction  $\delta^{18}\text{O}/\delta^{13}\text{C}$  and C/N ratio data for the RBS succession. The data are plotted against the same sedimentary log as used in Figures 3 and 4 to ease comparison, with the dashed line representing the K/Pg boundary.

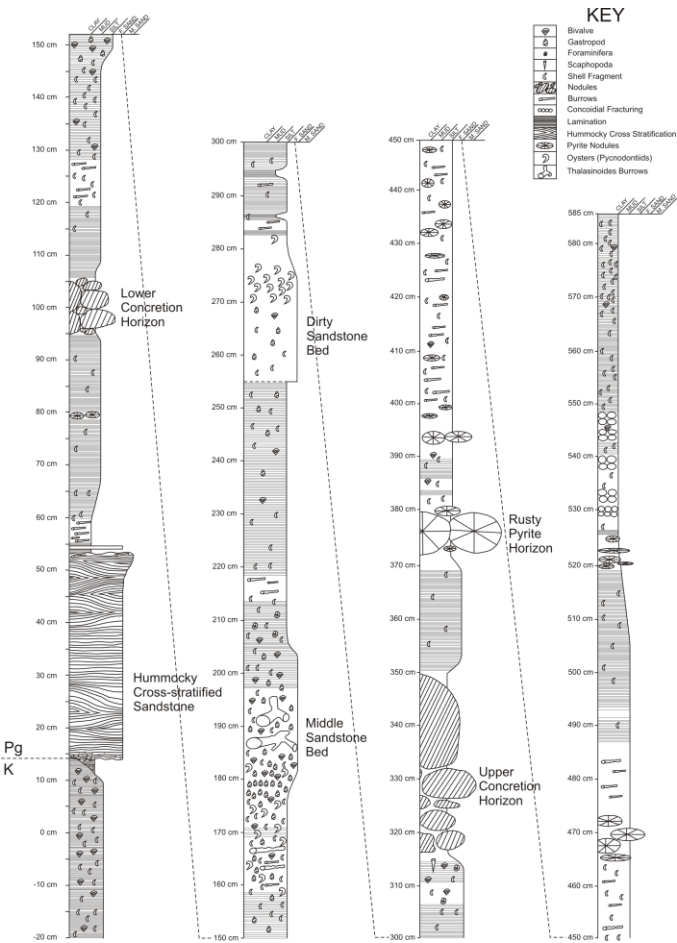
635



636

637 Figure 1. Locality map of the Brazos River area, Falls County, Texas (after Hart et al., 2012).

638



639

Figure 2. Sedimentary log of the K/Pg boundary succession exposed on the Brazos River at RBS (based on Hart et al., 2012). The thin volcanic ash recorded in the uppermost Maastrichtian of the Cottonmouth Creek succession (Hart et al., 2012) has not been recorded in the RBS succession, despite digging into the Maastrichtian mudstones as far as river levels allowed.

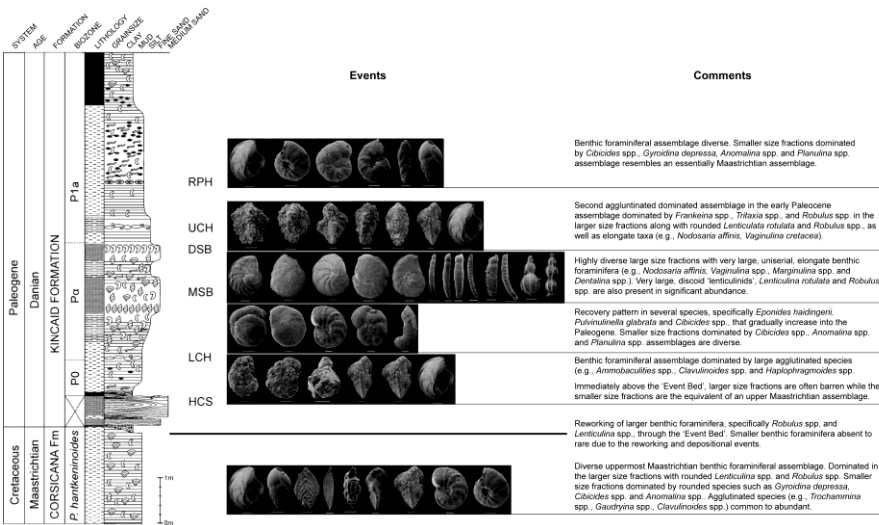


Figure 3. Sedimentary log of the RBS succession, which also shows examples of a representative selection of benthic foraminifera. The lithological symbols are explained in Figure 2 and the bed names follow Yancey (1996) including, from bottom to top, Hummocky Cross-Stratification (HCS), Lower Calcareous Horizon (LCH), Middle Sandstone Bed (MSB), Dirty Sandstone Bed (DSB), Upper Calcareous Horizon (UCH) and Rusty Pyrite Horizon (RPH).

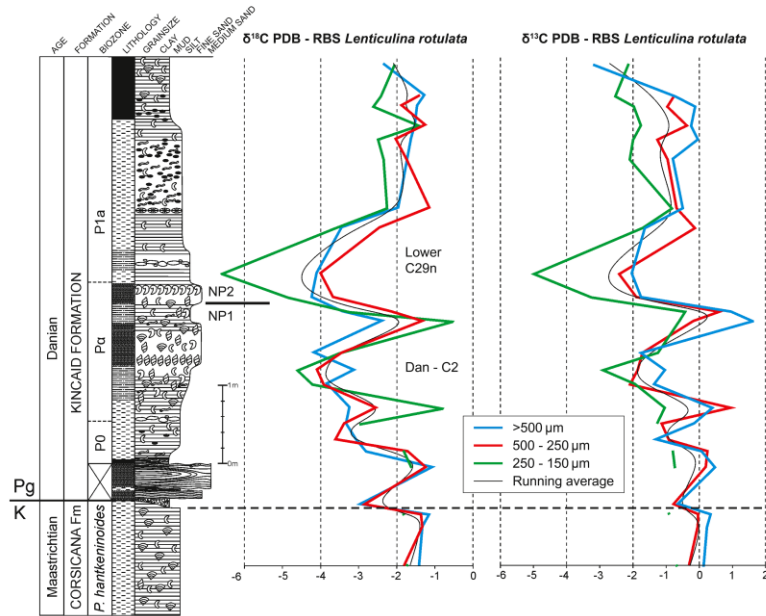


Figure 4. Comparison of the  $\delta^{18}\text{O}$  and  $\delta^{13}\text{C}$  stable isotope data derived from an analysis of *Lenticulina rotulata* Lamarck in the  $>500\ \mu\text{m}$ ,  $500\text{--}250\ \mu\text{m}$  and  $250\text{--}150\ \mu\text{m}$  size fractions. The thinner black line marks the running average.

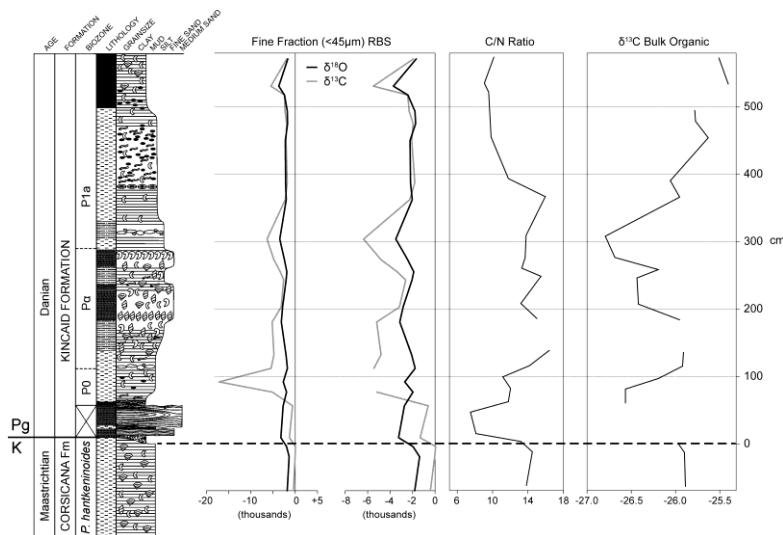


Figure 5. Bulk organic  $\delta^{13}\text{C}$ , fine fraction  $\delta^{18}\text{O}/\delta^{13}\text{C}$  and C/N ratio data for the RBS succession. The data are plotted against the same sedimentary log as used in Figures 3 and 4 to ease comparison, with the dashed line representing the K/Pg boundary.